articles

Tropical to mid-latitude snow and ice accumulation, flow and glaciation on Mars

J. W. Head[1], G. Neukum[2], R. Jaumann[3], H. Hiesinger[1], E. Hauber[3], M. Carr[4], P. Masson[5], B. Foing[6], H. Hoffmann[3], M. Kreslavsky[1], S. Werner[2], S. Milkovich[1], S. van Gasselt[2] & The HRSC Co-Investigator Team*

[1]Department of Geological Sciences, Brown University, Providence, Rhode Island 02912, USA
[2]Institut fuer Geologische Wissenschaften, Freie Universitaet Berlin, Malteserstrasse 74-100, Bldg D, 12249 Berlin, Germany
[3]DLR-Institut fuer Planetenforschung, Rutherfordstrasse 2, 12489, Berlin, Germany
[4]US Geological Survey, MS 975, Menlo Park, California 94025, USA
[5]Orsay-Terre, F-91405, Orsay Cedex, France
[6]ESTEC/SCI-SR, Postbus 299, NL2200AG Noordwijk, The Netherlands
*A list of all members of The HRSC Co-Investigator Team and their affiliations appears at the end of the paper

....

Images from the Mars Express HRSC (High-Resolution Stereo Camera) of debris aprons at the base of massifs in eastern Hellas reveal numerous concentrically ridged lobate and pitted features and related evidence of extremely ice-rich glacier-like viscous flow and sublimation. Together with new evidence for recent ice-rich rock glaciers at the base of the Olympus Mons scarp superposed on larger Late Amazonian debris-covered piedmont glaciers, we interpret these deposits as evidence for geologically recent and recurring glacial activity in tropical and mid-latitude regions of Mars during periods of increased spin-axis obliquity when polar ice was mobilized and redeposited in microenvironments at lower latitudes. The data indicate that abundant residual ice probably remains in these deposits and that these records of geologically recent climate changes are accessible to future automated and human surface exploration.

Among the most sensitive abiotic indicators of climate change are the accumulation, stability and flow of snow and ice. During the Little Ice Age on Earth (late sixteenth to early twentieth centuries), for example, glaciers at high latitude and altitude advanced an average of several kilometres[1] and today many are receding in concert with warming trends[2]. On Mars, shallow subsurface water-ice stability in the current climate is limited to latitudes higher than about 60°, a theoretical prediction[3] borne out by spacecraft observation[4]. At present the spin-axis obliquity of Mars, thought to be among the major factors in climate change, is about 25°, but calculations show that there were several periods of increasingly higher obliquity in the last several millions of years of the history of Mars[5]. General circulation models show that increased obliquity warms ice-rich polar regions and redistributes water-ice deposits equatorward[6–8]. Indeed, geological observations show evidence for a recent ice age in the last several million years in the form of a latitude-dependent dust–ice mantle extending from high latitudes down to about 30° latitude in both hemispheres[9], and evidence for localized tropical mountain glacier deposits that formed during earlier epochs of the Late Amazonian period on Mars tens to hundreds of millions of years ago[10]. Furthermore, there are numerous morphologic features that might involve ice-rich material at low to mid-latitudes throughout the history of Mars (such as landslides, debris aprons, rock glaciers and piedmont glaciers) but the origins, sources, amounts and state of water in these materials has been controversial[11–20].

Here we report on results from the High Resolution Stereo Camera (HRSC)[21] on board Mars Express that show evidence for (1) the presence of significant volumes of ice and glacial-like flow in massif-marginal deposits at low to mid-latitudes (east of Hellas basin), and (2) very young glacier deposits in equatorial regions (Olympus Mons), suggesting recent climate change. Together these deposits are testimony to the importance and scale of equatorward water redistribution during recent climate change, and to the high

likelihood of the presence of significant volumes of buried ice currently in low-latitude regions on Mars.

Glacial-like flow in debris aprons

Debris aprons are a class of geomorphic features seen in mid-latitudes of Mars that are hundreds of metres thick, slope gently away from scarps or highland massifs, terminate at lobate margins, and are interpreted to be viscous flow features of material containing some portion of lubricating ice derived from adjacent highlands[11]. New altimetry and high-resolution images have permitted more comprehensive observations and modelling but have not been able to distinguish conclusively among multiple models of apron formation[17] (for example, ice-assisted rock creep, ice-rich landslides, rock glaciers and debris-covered glaciers) because of our inability to determine the proportion of ice in the rock debris (which can range widely, from ice deposited in debris interstices to debris deposited on ice accumulations)[11–17]. Indeed, different aprons may have different modes of formation.

New HRSC data provide wide coverage of high-resolution data with a high signal-to-noise ratio and stereo capability. Analysis of new HRSC data of a massif-marginal lobe in the eastern Hellas region conclusively shows that the proportion of ice in this deposit was substantial enough to signify glacial and debris-covered glacial activity. Specifically, an 18-km-wide lobe extends about 8 km from the base of a 3.75-km-high massif (Fig. 1). The lobe is up to about 250 m thick, has a convex upward topographic profile, and is separated from the base of the massif by an irregular 50–100-m-deep depression (Fig. 1b, c). A broad alcove in the massif (Fig. 1a) adjacent to the lobe could be interpreted as a landslide scar, representing the source region for the lobate deposit. However, we find several inconsistencies with such an interpretation. For example, within the lobe itself (Fig. 1d), a distal 4-km zone is characterized throughout by a fretted and honeycomb-like texture of irregular pits and ridges. Depressions typically 20–40 m deep

make up 30–40% of this zone and occur between linear moraine-like ridges forming broad convex-outward lobes.

These patterns of sinuous ridges and irregular depressions are unlike landslides and are typical of Earth glacial deposits that remain following debris-containing glacial ice advance, stagnation and ablation[22]. Debris input to glaciers occurs most commonly at ice margins and is thus concentrated along the base of cirques and in medial debris septa that ultimately become medial moraines[23]. Proximal debris addition from rockfalls and increasing debris concentration from below by ice sublimation results in supraglacial debris mantles in the distal direction with great spatial variability in thickness and grain size. As ablation proceeds, debris accumulations represented by englacial septa emerge and form longitudinal or transverse debris ridges separated by areas of cleaner or bare ice. Continued ablation results in the downwasting of the cleaner ice to produce pits, dirt cones and topographic inversion between the ridges, and ultimately the emerging or redistributed debris becomes thick enough to retard further sublimation[24].

The morphological similarities of features observed in Fig. 1 to glacial deposits are thus suggestive of processes of snow and ice accumulation, viscous flows of debris-containing ice, and the subsequent sublimation of significant volumes of the ice in the deposit, leaving behind numerous large sublimation pits tens of metres deep and intervening morainal ridges. Towards the massif, the presence of the linear depression suggests that this may have been the region of snow and ice accumulation; the present depressed topography (with local pits approaching a depth of 100 m) may represent typical proximal high concentrations of ice where more complete sublimation would take place. The presence of numerous plateaus in the fretted part of the deposit suggests that substantial quantities of ice remain beneath a local debris-rich cover, while sublimation has removed intervening ice to produce fretted pits.

These relationships strongly suggest that rather than a landslide scar, the broad alcove represents an accumulation zone for snow and ice that incorporates debris from the massif and under appropriate accumulation conditions, flows out into the surrounding terrain. Although we can see evidence for older lobate deposits, no super-posed impact craters have been observed on this deposit, suggesting

a geologically recent age for this deposit. Despite its apparent recent age, the evidence for extensive sublimation and wasting are strong indicators that the current environment is not conducive to this large-scale accumulation and flow. However, the probable preservation of ice beneath a substantial portion of this deposit (underlying the sublimation till surface of the inter-pit plateaus) supports the probability that many of the other debris aprons also represent very ice-rich debris-covered glaciers. Indeed, theoretical predictions for Mars imply that dust can insulate buried ice[25] and observations in the Antarctic Dry Valleys suggest that sublimation tills can protect underlying glacial ice for millions of years[26].

Hour-glass-shaped flow in craters

Do other examples of debris aprons show features that might further distinguish between origins from ice-assisted rock creep, ice-rich landslides, rock glaciers and debris-covered glaciers?[11–17] We see further evidence for viscous flow of very ice-rich material in the HRSC data of an hourglass-shaped deposit occurring in two craters at the base of a 3.5–4-km-high massif located on the eastern rim of the Hellas basin (Fig. 2). Two adjacent circular depressions about 9 and 16 km in diameter extend outward from the base of the massif into the surrounding lowlands. In contrast to the previously described deposit, which was oriented with its long axis parallel to the massif slope (Fig. 1), in this location (Fig. 2) the deposit is contained within the craters and appears to fill them. In the proximal crater, the floor is a regionally flat surface that lies nearly at the rim, about 500 m above the surrounding plain, and along a N–S topographic profile (Fig. 2e) the crater appears to be filled nearly to the brim. E–W profiles show, however, that the floor tilts away from the massif at a slope of less than a few degrees (Fig. 2f).

The surface texture on the floor of the crater revealed by the HRSC data (Fig. 2c, d) shows unequivocal evidence for streamlines and lobes typical of ice flow and ice-lobe interaction. Four discrete zones are seen within this crater. To the north, arcuate nested lobes emerge fully developed from the base of the slope and are progressively compressed along the margin; these give way in the north-central part of the crater to a 2.5-km-wide zone of parallel ridges that converge to a narrower 1-km-wide zone where the rim of the
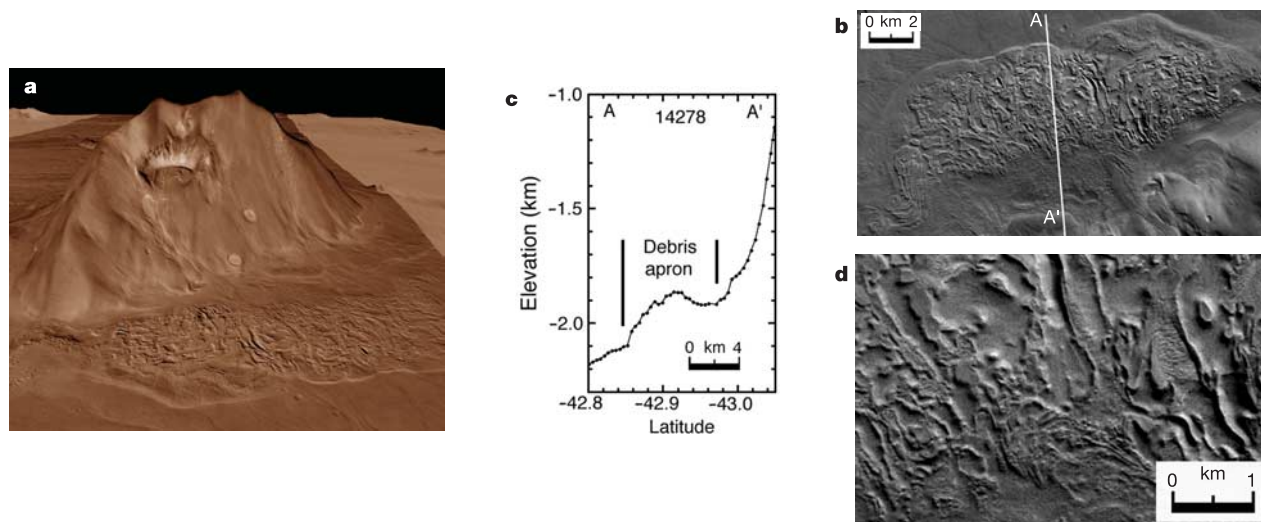
Figure 1 Massif and debris-apron deposits on the eastern rim of the Hellas basin (262.8° W, −43.2°). All images are portions of MEX HRSC Orbit 300. **a**, Perspective view looking east of the 3.75-km-high massif surrounded by debris aprons. Vertical exaggeration is ~30×. **b**, Debris apron with a significant portion comprised of fretted pits and depressions, suggesting the former presence of ice. Line shows location of MOLA profile A–A′. **c**, Altimetric profile across base of massif and debris-apron deposit. MOLA orbit 14278. **d**, Enlargement of portion of fretted debris-apron deposit located just to the right of the profile (Fig. 1b). Note the lobate shapes and the presence of lateral and arcuate ridges and central depressions.

proximal crater is breached. A south central 1.5-km-wide zone of tight arcuate lobes points downslope and becomes compressed into parallel flowlines as it reaches the distal breach. In the southern part of the crater, a 3-km-wide zone of parallel ridges is progressively compressed into a very narrow zone less than 1 km in width. All four of these zones join together at the low point in the crater rim, and flow through a narrow breach less than 2 km wide (Fig. 2d), dropping several hundred metres in elevation and spreading out onto the lower crater floor, creating a set of lobate ridges and depressions further indicative of viscous flow. This configuration is very similar to Earth glacial environments, such as the 60-km-wide Malispina glacier[27], where parallel ridges form due to low-viscosity, high-strain-rate flow in narrow valley glaciers; these then emerge out onto a broad plain and spread out to form a piedmont glacier many times the width of the initial constriction.

The viscous-flow-like crater-filling materials appear to be fully developed at the proximal end of the smaller crater adjacent to the massif alcove (Fig. 2a–d). Here too, the distinctive alcove in the massif could, in principle, represent a landslide scar. Examination of the alcove area details, however, reveals evidence for individual topographic lineations and depressions favouring the accumulation and flow of ice, rather than landslides[20]. In summary, the nature, morphology and topography of the deposit indicates that the alcove served as an accumulation zone for snow and ice that acquired a debris cover from the surrounding steep slopes, and flowed out from the base of the alcove into the surrounding depressions, filling the proximal one and then breaching and overflowing to fill the lower depression. Further evidence that the viscously flowing material was predominantly ice comes from (1) the expanded lobate and complexly deformed nature of the deposit as it spreads out onto the floor of the lower crater from the notch in the upper crater (Fig. 2a, b), (2) the abundance of irregular-shaped pits in the distal lobes, indicating ice sublimation (Fig. 2a, b), (3) evidence for distal moraines around the crater interior margins, indicating ice retreat (Fig. 2b), and (4) compressed and deformed ridges and elongated craters (Mars Orbiter Camera (MOC) image M2300829) also suggest an ice-like rheology (Fig. 2c, d). We thus interpret these features to be debris-covered piedmont-type glaciers.
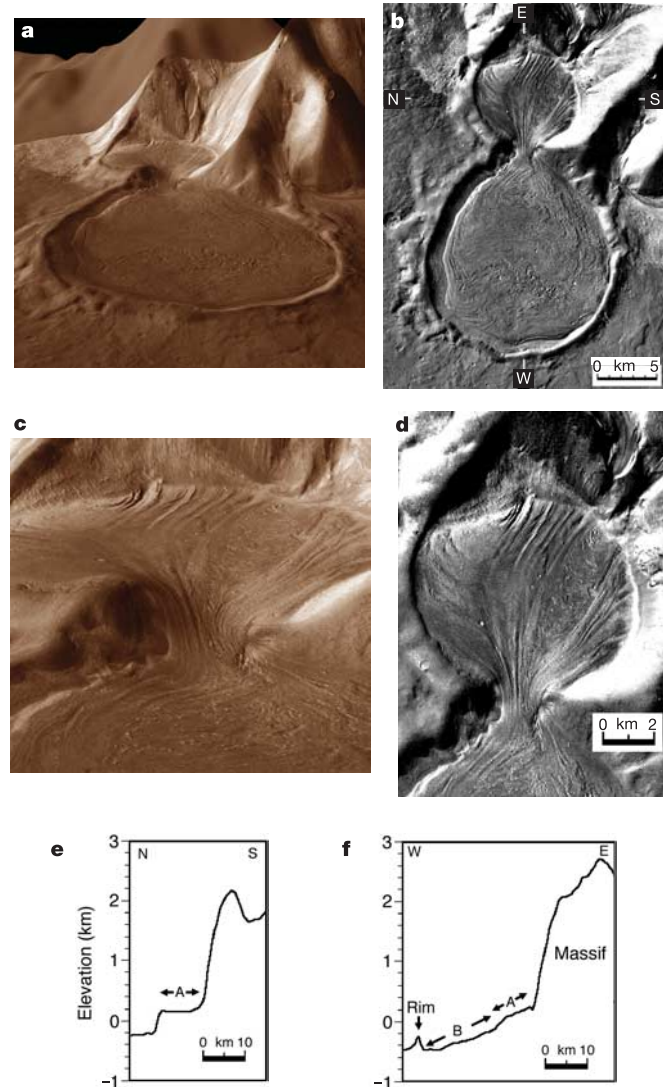
Young rock glaciers at Olympus Mons

Evidence for extensive debris-covered piedmont glaciers along the northwest edge of the Olympus Mons scarp has been described from Viking and THEMIS data[20,28,29], and together with the tropical mountain glaciers at the Tharsis Montes[10,30], they stand as evidence of extensive localized glaciation in the Late Amazonian when obliquity was typically[5] in excess of 35°. These glaciers extend up to 70–120 km from the base of the Olympus Mons scarp[28,29] and over 350 km from Arsia Mons[10].

HRSC data reveal the presence of several additional rock-glacier-like features along the Olympus Mons basal scarp that are clearly superposed on top of the larger, and thus older, debris-covered piedmont glaciers (Fig. 3). Here the individual lobes are about 25 km in length, and much narrower than the piedmont glacier
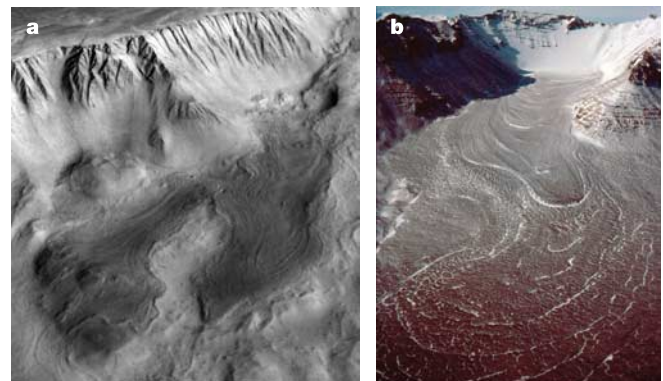

Figure 2 Hourglass-shaped deposit at the base of a massif on the eastern Hellas basin rim (257° W, −39.2°). All images are from MEX HRSC orbit 248. **a**, Perspective view of the 3.5–4-km-high massif showing viscous flow of material from a 9-km crater (marked A in Fig. 2e, f) through a narrow notch into a 16-km-diameter crater (marked B in Fig. 2f). Vertical exaggeration is ∼30×. **b**, Vertical view of the two craters showing flowlines and lobes. Tickmarks show the location of MOLA gridded topography profiles in **e** and **f**. **c**, Enlargement of the notch between the two craters showing the four zones where flowlines starting at the base of the slope converge at the narrow 2-km-wide notch and then diverge and spread laterally out into the lobate deposits below. **d**, Perspective view of the proximal crater showing flowlines converging in the gap. MOLA gridded altimetric profiles N–S (**e**) and E–W (**f**).

Figure 3 Deposits from a recent lobate rock glacier at the base of the Olympus Mons scarp (138° W, 18°). **a**, Perspective view looking southwest towards the 6-km-high scarp. Note lobate deposits extending about 20–25 km from the base of the alcoves (from right centre towards lower left) darkened for emphasis. HRSC data from MEX orbit 143. **b**, Perspective view of the upper ∼5 m of a debris-covered rock glacier emerging from a cirque in Mullins Valley, Antarctic Dry Valleys on Earth. Note the morphologic similarity to features at the base of Olympus Mons. Photo courtesy of David Marchant.

deposit on which they are superposed (Fig. 3a). Furthermore, the paths of the lobes closely follow the topography of the pre-existing deposit, an indication that they are the result of material advancing from the base outward, and not just backwasting and retreat of the residual larger lobe. The sources of the lobes are cuspate alcoves in the basal scarp (Fig. 3a), topographic depressions that are natural traps for wind-blown snow in terrestrial rock glacier environments[31–33] (Fig. 3b). Previously, the broad lobate features had been interpreted to be landslides[34], but terrestrial analogues[20] and new data[10,28–30] have provided very strong evidence for a debris-covered piedmont glacier origin. The new HRSC data add further support to the general glacial interpretation; evidence supporting a rock glacier interpretation for these smaller lobate features includes (1) their origin in alcoves, (2) their elongated subparallel concentric ridges, distorted in relation to underlying and adjacent topography, (3) distinctive terminal moraines, and (4) their strong morphological similarities to terrestrial rock glaciers of known glacial origin[10,30–32] (compare Fig. 3a, b).

Thus, we conclude that there is clear evidence for the formation

of recent rock glaciers locally at the base of the Olympus Mons scarp (Fig. 3), similar to typical rock glaciers formed in cirques in the Antarctic Dry Valleys, and their recent advance on Mars to distances measured in several tens of kilometres. The lack of snow in the present alcove, evidence of a depression there, and the presence of fans of scarp talus spreading downslope into these regions with no evidence of gelifluction (the slow downslope movement of sediment associated with seasonal thawing of ground ice), are all evidence that the young rock glaciers are no longer active and that the snow-accumulation conditions that led to their formation no longer persist in this area of Mars.

Role of glaciation in debris-apron origin

Previously, significant controversy surrounded the origin of debris aprons at the base of many massifs on Mars. Outstanding questions focused on (1) the abundance of ice in the deposits during formation, (2) the origin of this ice ('bottom up', from ground ice or groundwater, or 'top down', from atmospheric frost or snow accumulation), and (3) the mode of origin of these features (ranging
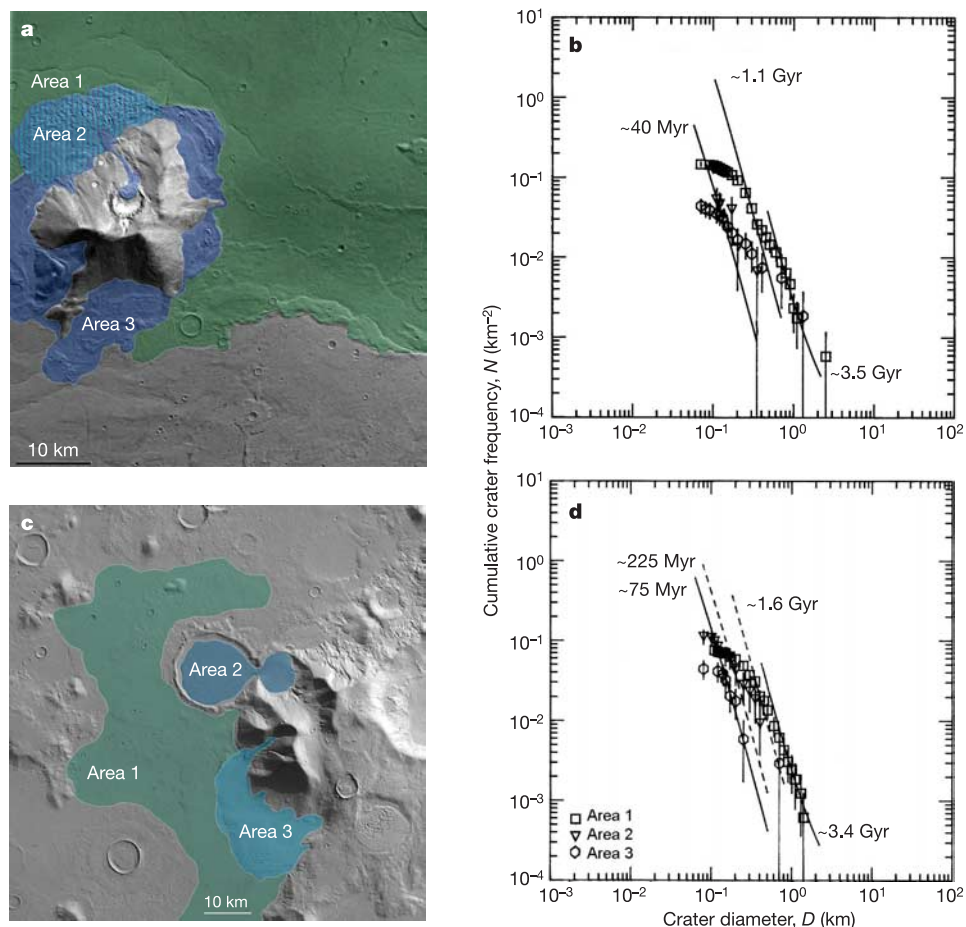

Figure 4 Ages of events in the lobate debris aprons. The impact-crater size-frequency distribution[37–39] has been fitted to individual segments of the distribution, giving values for the different episodes; application of the Hartmann–Neukum cratering chronology provides absolute ages. For ages younger than ~3 Gyr the error is around 20–30%. Error bars are one-sigma. All ages <2 Gyr may be affected in the same way by a possible systematic error of ~2× in the cratering model used[39]. **a**, **b**, Massif and fretted debris apron (**a** and Fig. 1), and impact crater size-frequency distributions (**b**). Area 1, surrounding the massif and lobate deposit, has an age of 3.5 Gyr and appears to have been resurfaced as late as 1.1 Gyr ago, due in part to fluvial activity represented by numerous channels. Debris aprons surrounding the massif (area 3 combined with area 2) display evidence for almost continuous erosion. The portion of the debris apron deposit

represented by the fretted debris apron (area 2) is as young as 40 Myr. If debris apron fretting is due to ice sublimation and the sublimation process was continuous over millions of years, some impact craters might be lost and therefore 40 Myr would be a minimum age. Crater distributions are from HRSC orbit 300 data. **c**, **d**, Hourglass structure apron (**c** and Fig. 2), and impact crater size-frequency distributions (**d**). The area surrounding the hourglass and lobate deposit (area 1) has an age of 3.4 Gyr and appears to have been almost continuously resurfaced, with a pause at ~1.4 Gyr, and with some indication of a resurfacing event ending about 225 Myr ago (second dashed line). The hourglass deposit (area 2) and the adjacent debris apron to the south (area 3) have a well-defined age of 75 Myr. Crater distributions are from HRSC orbit 248 data.

from ice-assisted rock creep, ice-rich landslides, rock glaciers, to debris-covered glaciers)[11–17]. HRSC data provide important new evidence relevant to each of these outstanding questions. First, the HRSC data support a dominant role for ice in the formation of some of these debris aprons and related deposits with evidence from the pitted terrain indicating very high proportions of ice in a debris apron (Fig. 1b, d), and evidence for low-viscosity flow in the hourglass-like feature, indicating high ice–debris ratios (Fig. 2). Second, evidence for the very high abundance of ice in the deposits and hyperarid cold polar-desert-like conditions during formation argues against bottom-up sources such as groundwater, and favours top-down sources, such as atmospheric-related processes of frost, snow or ice accumulation. Third, the proximity of the source regions for these features to steep-sided debris-covered alcoves, and their close analogue to areas on Earth where snow accumulates to form debris-covered, viscously flowing ice deposits (glaciers) (Fig. 3), strongly suggests that many of these features originate as extremely ice-rich, debris-covered glaciers. The geometry of the features discovered along the base of the Olympus Mons scarp, their similar origin in alcoves, their similarities in size and morphology to terrestrial debris-covered ice-rich rock glaciers, and their direct superposition on larger deposits interpreted to be Late Amazonian debris-covered piedmont glaciers[28,29] all strengthen the interpretation of the potential importance of glacial activity in the formation and evolution of debris aprons surrounding massifs on Mars.

Conclusions and implications

The presence of significant volumes of ice and glacial-like flow in massif-marginal deposits at low to mid-latitudes on Mars (east of Hellas basin; $-39°$ to $-43°$ latitude) and in rock glaciers at the base of Olympus Mons ($+18°$) strongly suggests that conditions in the geological past have favoured the accumulation of snow and ice and its flow in these tropical and mid-latitude regions. Crater size-frequency distribution data collected from the HRSC images (Fig. 4) of the lobate debris aprons east of Hellas (Figs 1, 2) show evidence for multiple eras of ice-related resurfacing, while the Olympus Mons rock glaciers (Fig. 3) are just a few million years old[35]. Thus, these deposits are further testimony to the importance and scale of equatorward water redistribution during climate change[6–8], and its accumulation in specific areas[35,36]. Furthermore, the super-position of the Olympus Mons rock glaciers on older debris-covered piedmont glacier deposits[28–29], dated at 280 to 130 million years (Myr) ago for the major lobes[36], strongly suggests that these conditions fluctuate with time, and that the geologically very young Olympus Mons rock glaciers documented here (Fig. 3a) represent a recent return to these conditions a few million years ago[36] for periods shorter than those that formed the underlying, much more extensive, Late Amazonian deposits. Finally, that none of these features at present seem to be accumulating ice, and thus flowing and advancing, but instead appear to be undergoing sublimation and wasting, strongly suggests that conditions conducive to their formation are not currently in effect. The latter point is consistent with the idea that Mars may now be in an 'interglacial' period due to its relatively low obliquity[9]. Thus, deposits such as these revealed in detail by the HRSC data provide an important geological record of recent climate change that can be used to test and improve both models of recent climate change[6–8] and predictions of the history of orbital parameters[5]. The lower latitudes of these ice-rich deposits also mean that this key climate record is very accessible to automated and human exploration for direct examination and analysis. □

1. Grove, J. M. *The Little Ice Age* (Routledge, London, 1988).
2. Warren, C. R. Glaciers in the greenhouse. *Geogr. Rev.* **8,** 2–7 (1995).
3. Mellon, M. T. & Jakosky, B. M. The distribution and behavior of Martian ground ice during past and present epochs. *J. Geophys. Res.* **100,** 11781–11799 (1995).
4. Feldman, W. C. *et al.* Global distribution of neutrons from Mars: Results from Mars Odyssey. *Science* **297,** 75–78 (2002).
5. Laskar, J. *et al.* Long term evolution and chaotic diffusion of the insolation quantities of Mars. *Icarus* **170,** 343–364 (2004).
6. Richardson, M. I. & Wilson, R. J. Investigation of the nature and stability of the Martian seasonal water cycle with a general circulation model. *J. Geophys. Res.* **107,** doi:10.1029/2001JE001536 (2002).
7. Mischna, M. *et al.* On the orbital forcing of Martian water and CO_2 cycles: A general circulation model study with simplified volatile schemes. *J. Geophys. Res.* **108,** doi:10.1029/2003JE002051 (2003).
8. Haberle, R. M. *et al.* Orbital change experiments with a Mars general circulation model. *Icarus* **161,** 66–89 (2003).
9. Head, J. W. *et al.* Recent ice ages on Mars. *Nature* **426,** 797–802 (2003).
10. Head, J. W. & Marchant, D. R. Cold-based mountain glaciers on Mars: Western Arsia Mons. *Geology* **31,** 641–644 (2003).
11. Squyres, S. W. Martian fretted terrain—Flow of erosional debris. *Icarus* **34,** 600–613 (1978).
12. Colaprete, A. & Jakosky, B. M. Ice flow and rock glaciers on Mars. *J. Geophys. Res.* **103,** 5897–5909 (1998).
13. Mangold, N. & Allemand, P. Topographic analysis of features related to ice on Mars. *Geophys. Res. Lett.* **28,** 407–410 (2001).
14. Mangold, N. *et al.* Experimental and theoretical deformation of ice-rock mixtures: Implications on rheology and ice content of Martian permafrost. *Planet. Space Sci.* **50,** 385–401 (2002).
15. Baratoux, D. *et al.* Evidence of liquid water in recent debris avalanche on Mars. *Geophys. Res. Lett.* **29,** doi:10.1029/2001GL014155 (2002).
16. Mangold, N. Geomorphic analysis of lobate debris aprons on Mars at Mars Orbiter Camera scale: Evidence for ice sublimation initiated by fractures. *J. Geophys. Res.* **108,** doi:10.1029/2002JE001885 (2003).
17. Pierce, T. L. & Crown, D. A. Morphologic and topographic analyses of debris aprons in the eastern Hellas region, Mars. *Icarus* **163,** 46–65 (2003).
18. Kargel, J. S. & Strom, R. G. Ancient glaciation on Mars. *Geology* **20,** 3–7 (1992).
19. Baker, V. R. *et al.* Ancient oceans, ice sheets and the hydrological cycle on Mars. *Nature* **352,** 589–594 (1986).
20. Lucchitta, B. K. Mars and Earth—Comparison of cold-climate features. *Icarus* **45,** 264–303 (1981).
21. Neukum, G. *et al.* HRSC: *The High Resolution Stereo Camera of Mars Express* 17–35 (Report ESA-SP-1240, European Space Agency Publications Division, Noordwijk, The Netherlands, 2004).
22. Benn, D. I. & Evans, D. J. A. *Glaciers and Glaciation* 237–239 (Arnold, London, 1998).
23. Eyles, N. & Rogerson, R. J. A framework for the investigation of medial moraine formation: Austerdalsbreen, Norway, and Berendon Glacier, British Columbia, Canada. *J. Glaciol.* **20,** 99–113 (1978).
24. Boulton, G. S. in *Till: A Symposium* (ed. Goldthwait, R. P.) 41–72 (Ohio State Univ. Press, Columbus, 1971).
25. Skorov, Yu. V. *et al.* Stability of water ice under a porous nonvolatile layer: implications to the south pole layered deposits of Mars. *Planet. Space Sci.* **49,** 59–63 (2001).
26. Marchant, D. *et al.* Formation of patterned ground and sublimation till over Miocene glacier ice in Beacon Valley, southern Victoria Land, Antarctica. *Geol. Soc. Am. Bull.* **114,** 718–730 (2002).
27. Hartshorn, J. H. Supraglacial and proglacial geology of the Malaspina Glacier, Alaska, and its bearing on glacial features of New England. *Geol. Soc. Am. Bull.* **63,** 1259–1260 (1952).
28. Milkovich, S. M. & Head, J. W. Olympus Mons fan shaped deposit morphology: Evidence for debris glaciers. *6th Int. Mars Conf.* abstr. 3149 (2003).
29. Head, J. W., Shean, D. E., Milkovitch, S. M. & Marchant, D. Tropical mountain glaciers on Mars: Evidence for Amazonian climate change. *3rd Mars Polar Conf.* abstr. 8105 (2003).
30. Shean, D. E. *et al.* Tharsis Montes cold-based glaciers: Observations and constraints for modeling and preliminary results. *Lunar Planet. Sci.* **XXXV,** abstr. 1438 (2004).
31. Potter, N. Periglacial geomorphology. *J. Geol. Educ.* **32,** 226–232 (1984).
32. Johnson, P. G. Glacier-rock glacier transition in the southwest Yukon Territory. *Arctic Alpine Res.* **12,** 195–204 (1980).
33. Martin, H. E. & Whalley, W. B. Rock glaciers, part 1, Rock glacier morphology: Classification and distribution. *Prog. Phys. Geogr.* **11,** 260–282 (1987).
34. Morris, E. C. & Tanaka, K. L. *Geologic Maps of the Olympus Mons Region of Mars* (Map I-2327, Misc. Inv. Ser., US Geological Survey, Reston, Virginia, 1994).
35. Neukum, G. *et al.* Recent and episodic volcanic and glacial activity on Mars revealed by the High Resolution Stereo Camera. *Nature* **432,** 971–979 (2004).
36. Hauber, E. *et al.* Discovery of a flank caldera and very young glacial activity at Hecates Tholus, Mars. *Nature* doi:10.1038/nature03423 (this issue).
37. Neukum, G. *et al.* Cratering record in the inner Solar System in relation to the lunar reference system. *Space Sci. Rev.* **96,** 55–86 (2001).
38. Ivanov, B. A. Mars/Moon cratering rate ratio estimates. *Space Sci. Rev.* **96,** 87–104 (2001).
39. Hartmann, W. K. & Neukum, G. Cratering chronology and the evolution of Mars. *Space Sci. Rev.* **96,** 165–194 (2001).

Correspondence and requests for materials should be addressed to J.W.H. (james_head@brown.edu).

The HRSC Co-Investigator Team: J. Albertz[1], A. T. Basilevsky[2], G. Bellucci[3], J.-P. Bibring[4], M. Buchroithner[5], M. H. Carr[6], E. Dorrer[7], T. C. Duxbury[8], H. Ebner[9], B. H. Foing[10], R. Greeley[11], E. Hauber[12], J. W. HeadIII[13], C. Heipke[14], H. Hoffman[12], A. Inada[15,18], W.-H. Ip[16], B. A. Ivanov[17], R. Jaumann[12], H. U. Keller[18], R. Kirk[19], K. Kraus[20], P. Kronberg[21], R. Kuzmin[2], Y. Langevin[4], K. Lumme[22], W. Markiewicz[18], P. Masson[23], H. Mayer[7], T. B. McCord[24], J.-P. Muller[25], J. B. Murray[26], F. M. Neubauer[27], G. Neukum (Principal Investigator)[28], J. Oberst[12], G. G. Ori[29], M. Pätzold[27], P. Pinet[30], R. Pischel[12], F. Poulet[4], J. Raitala[31], G. Schwarz[32], T. Spohn[12] & S. W. Squyres[33]

Affiliations of authors: 1, TU Berlin, D-10623 Germany; 2, Vernadsky Institute-RAS, Moscow 117975, Russia; 3, CNR/IFSI, 00133 Rome, Italy; 4, CNRS/IAS, 91405 Orsay Cedex, France; 5, TU Dresden, D-01062 Germany; 6, USGS, MS 975 Menlo Park, California 94025, USA; 7, Universität der Bundeswehr München, D-85577 Neubiberg, Germany; 8, JPL, Pasadena, California 91109, USA; 9, TU München, D-80333 Germany; 10, ESTEC/SCI-SR, Postbus 299, NL-2200 AG Noordwijk, The Netherlands; 11, Arizona State University, Box 871404, Tempe, Arizona 85287-1404, USA; 12, DLR, D-12489 Berlin, Germany; 13, Brown University, Box 1846, Providence, Rhode Island 02912, USA; 14, Universität Hannover, D-30167 Germany; 15, Kobe University, 657-8501 Kobe, Japan; 16, National Central University (NCU), Chung-Le 320 Taiwan; 17, IDG-RAS, Moscow 117979, Russia; 18, MPAE, Postfach 20, D-37191 Katlenberg-Lindau, Germany; 19, USGS, Flagstaff, Arizona 86001; 20, TU Wien, A-1040 Wien, Austria; 21, TU Clausthal, D-38678 Clausthal, Germany; 22, University of Helsinki, PO Box 14, SF-00014 Helsinki, Finland; 23, Orsay Terre, F-91405 Orsay Cedex, France; 24, PSI-Nw, Winthrop, Washington 98862, USA; 25, University College London WC1E 6BT, UK; 26, The Open University, Milton Keynes MK7 6AA Buckinghamshire, UK; 27, Universität Köln, D-50923 Germany; 28, FU Berlin, D-12249, Germany; 29, IRSPS, I-65127 Pescara, Italy; 30, Observatoire de Midi-Pyrénées, F-31400 Toulouse, France; 31, University of Oulu, FIN-90401 Finland; 32, DLR, D-82234 Wessling, Germany; 33, Cornell University, Ithaca, New York 15853-1301, USA